Part B for ScholarWorks@UA collection
Moment tensors for the mainshock and aftershocks of the 2018-11-30 M_w 7.1 Anchorage earthquake

Cole Richards and Carl Tape

May 15, 2019

Attribution: If you use these files, please cite *Richards* (2019) and *West et al.* (2019). This document is downloadable as a pdf via the link listed in *Richards* (2019). This is Part B of the collection; see also Part A, which focuses on the aftershocks.

Description of files

A summary of files in the collection is listed in the following table:

file name	description
scholarworks_mshock.pdf	this file: summary of collection, including, depth tests, beachballs, and subsets of waveform fits for double couple and full moment tensor solutions
waveform_fits_mshock_DC.pdf	all station waveform fits for the double couple moment tensor solution
waveform_fits_mshock_fmt.pdf	all station waveform fits for the full moment tensor solution
weight_mshock.zip	zipped set of text files of input parameters for moment tensor inversions with all stations

Methods and Results

We use long-period regional seismic waveforms to estimate point-source moment tensor for the 2018-11-30 M_w 7.1 Anchorage earthquake. For the selection bandpass periods of 40–200 s, the waveforms can be well-modeled assuming a simple layered model of Earth structure and a point source representation for the earthquake. Our moment tensor approach is described in *Silwal and Tape* (2016) and uses a modified version of the 'cut-and-paste' (CAP) code (*Zhu and Helmberger*, 1996; *Zhu and Ben-Zion*, 2013). We calculate synthetic seismograms using the frequency-wavenumber approach (*Zhu and Rivera*, 2002) and the standard 1D model used in southern Alaska for earthquake location and moment tensor estimation (*Silwal and Tape*, 2016, Table S1). For the 2018 earthquake we use 106 stations. We generate a large number of uniformly distributed moment tensors, then evaluate a waveform misfit function between recorded and synthetic seismograms, and then save the moment tensor that provides the lowest misfit (i.e., best waveform fits).

A moment tensor is a 3×3 symmetric matrix that contains interpretable parameters. Its three eigenvalues define its magnitude and its source type. The source type can be defined in terms of a longitude angle γ and latitude angle δ in eigenspace (*Tape and Tape*, 2012). For a double couple, $\gamma = 0°$ and $\delta = 0°$; for a CLVD, $\gamma = \pm 30°$ and $\delta = 0°$. For an explosion or

implosion, $\gamma = 0^\circ$ and $\delta = \pm 90^\circ$. The remaining three parameters are the strike, dip, and rake angles; these describe the orientation of the moment tensor.

We perform two grid searches over the space of moment tensors and depths. In the first search, we constrain the moment tensor to be a double couple, which is equivalent to assuming that the earthquake ruptured on a single plane. In the second case, we search the full space of moment tensors (e.g., *Alvizuri and Tape*, 2016; *Alvizuri et al.*, 2018). For each case, after we establish the best-fitting depth, we perform an additional grid search using $\Delta M_{\mathrm{w}} = 0.01$ in order to obtain a more precise magnitude estimate. As we would expect, the waveform fits are quantitatively better in the case where a larger parameter space is allowed (i.e., FMT). The full moment tensor solution contains a small negative isotropic component; a more extensive analysis is needed to investigate whether this result is statistically significantly different from the best-fitting double couple.

The choice of moment tensor constraint (DC, deviatoric, FMT) will impact other source parameters, notably depth and magnitude, but also the orientation. For example, in our case, constraining the moment tensor to be a DC changes the depth from 45.2 to 50.2 km and the magnitude from 7.07 to 7.09 (Table M1).

In Table M1 we compare our two moment tensor results with those from GCMT (*Dziewonski et al.*, 1981; *Ekström et al.*, 2012) and USGS W phase (*Duputel et al.*, 2012). Both the GCMT and USGS moment tensors allow for deviatoric moment tensors, which are non-double-couple but have zero isotropic component (i.e., lune latitude 0°). For calculating the GCMT quantities in Table M1, we start with the M_{ij} entries provided in the CMTSOLUTION file. For the USGS quantities, we start with the M_{ij} entries in the netcdf file. Seismic moment is calculated via $M_0 = \|\mathbf{M}\|/\sqrt{2}$, and moment magnitude M_{w} is calculated via *Kanamori* (1977). The minor differences between the USGS and GCMT moment tensor solutions could arise from different waveforms (different stations, time windows, seismic phases, bandpass filters) and different 1D Earth models.

The long-period seismic radiation used in estimating the moment tensors in Table M1 indicates a source mechanism that is close to a double couple. The two possible fault planes are either east-dipping 30° or west-dipping 60°. The depth is 45–50 km and clearly within the subducting Pacific plate (*Hayes et al.*, 2018). Further analysis is needed to determine the significance of the small (negative: $\delta = -8.0^\circ$) isotropic component estimated from our full moment tensor inversion.

Table M1: Comparison of moment tensor depths, magnitudes, and source types. The AEC catalog depth is 46.7 km. The angle $\theta_{\rm dc}$ is the angle in matrix space (and on the lune) between a moment tensor and its closest double couple.

reference	depth km	mag. $M_{\rm w}$	lune long.	lune lat.	$\theta_{\rm dc}$	strike	dip	rake	strike	dip	rake
this study (DC)	50.2	7.09	0	0	0	191.3	60.8	-84.7	0.6	29.6	-99.3
this study (FMT)	45.2	7.07	-2.7	-8.0	8.5	187.8	62.4	-88.9	5.6	27.6	-92.0
GCMT - prelim	53.8	7.063	-6.4	0	6.4	190.3	60.4	-88.2	6.7	29.6	-93.2
GCMT	48.2	7.054	-5.1	0	5.1	188.7	63.6	-89.4	7.3	26.4	-91.3
USGS (W phase)	45.5	7.048	-4.8	0	4.8	189.4	62.2	-88.5	6.2	27.8	-92.9

References

Alvizuri, C., and C. Tape (2016), Full moment tensors for small events ($M_w < 3$) at Uturuncu volcano, Bolivia, *Geophys. J. Int.*, *206*, 1761–1783, doi:10.1093/gji/ggw247.

Alvizuri, C., V. Silwal, L. Krischer, and C. Tape (2018), Estimation of full moment tensors, including uncertainties, for nuclear explosions, volcanic events, and earthquakes, *J. Geophys. Res. Solid Earth*, *123*, 5099–5119, doi:10.1029/2017JB015325.

Duputel, Z., L. Rivera, H. Kanamori, and G. Hayes (2012), W phase source inversion for moderate to large earthquakes, *Geophys. J. Int.*, *189*, 1125–1147.

Dziewonski, A., T.-A. Chou, and J. H. Woodhouse (1981), Determination of earthquake source parameters from waveform data for studies of global and regional seismicity, *J. Geophys. Res.*, *86*(B4), 2825–2852, doi:10.1029/JB086iB04p02825.

Ekström, G., M. Nettles, and A. M. Dziewoński (2012), The global GCMT project 2004–2010: Centroid-moment tensors for 13,017 earthquakes, *Phys. Earth Planet. Inter.*, *200-201*, 1–9, doi:10.1016/j.pepi.2012.04.002.

Hayes, G. P., G. L. Moore, D. E. Portner, M. Hearne, H. Flamme, M. Furtney, and G. M. Smoczyk (2018), Slab2, a comprehensive subduction zone geomety model, *Science*, doi:10.1126/science.aat4723.

Kanamori, H. (1977), The energy release in great earthquakes, *J. Geophys. Res.*, *82*, 2981–2987.

Richards, C. (2019), Moment tensors for the mainshock and aftershocks of the 2018-11-30 M_w 7.1 Anchorage earthquake, ScholarWorks@UA at `http://hdl.handle.net/11122/10173` (last accessed 2019-05-16): descriptor files, text file of catalog, and figures of waveform fits.

Silwal, V., and C. Tape (2016), Seismic moment tensors and estimated uncertainties in southern Alaska, *J. Geophys. Res. Solid Earth*, *121*, 2772–2797, doi:10.1002/2015JB012588.

Tape, W., and C. Tape (2012), A geometric setting for moment tensors, *Geophys. J. Int.*, *190*, 476–498, doi:10.1111/j.1365-246X.2012.05491.x.

West, M. E., et al. (2019), The 30 November 2018 Mw 7.1 Anchorage earthquake, *Seismol. Res. Lett.* (in review).

Zhu, L., and Y. Ben-Zion (2013), Parameterization of general seismic potency and moment tensors for source inversion of seismic waveform data, *Geophys. J. Int.*, *194*, 839–843, doi:10.1093/gji/ggt137.

Zhu, L., and D. Helmberger (1996), Advancement in source estimation techniques using broadband regional seismograms, *Bull. Seismol. Soc. Am.*, *86*(5), 1634–1641.

Zhu, L., and L. A. Rivera (2002), A note on the dynamic and static displacements from a point source in multilayered media, *Geophys. J. Int.*, *148*, 619–627, doi:10.1046/j.1365-246X.2002.01610.x.

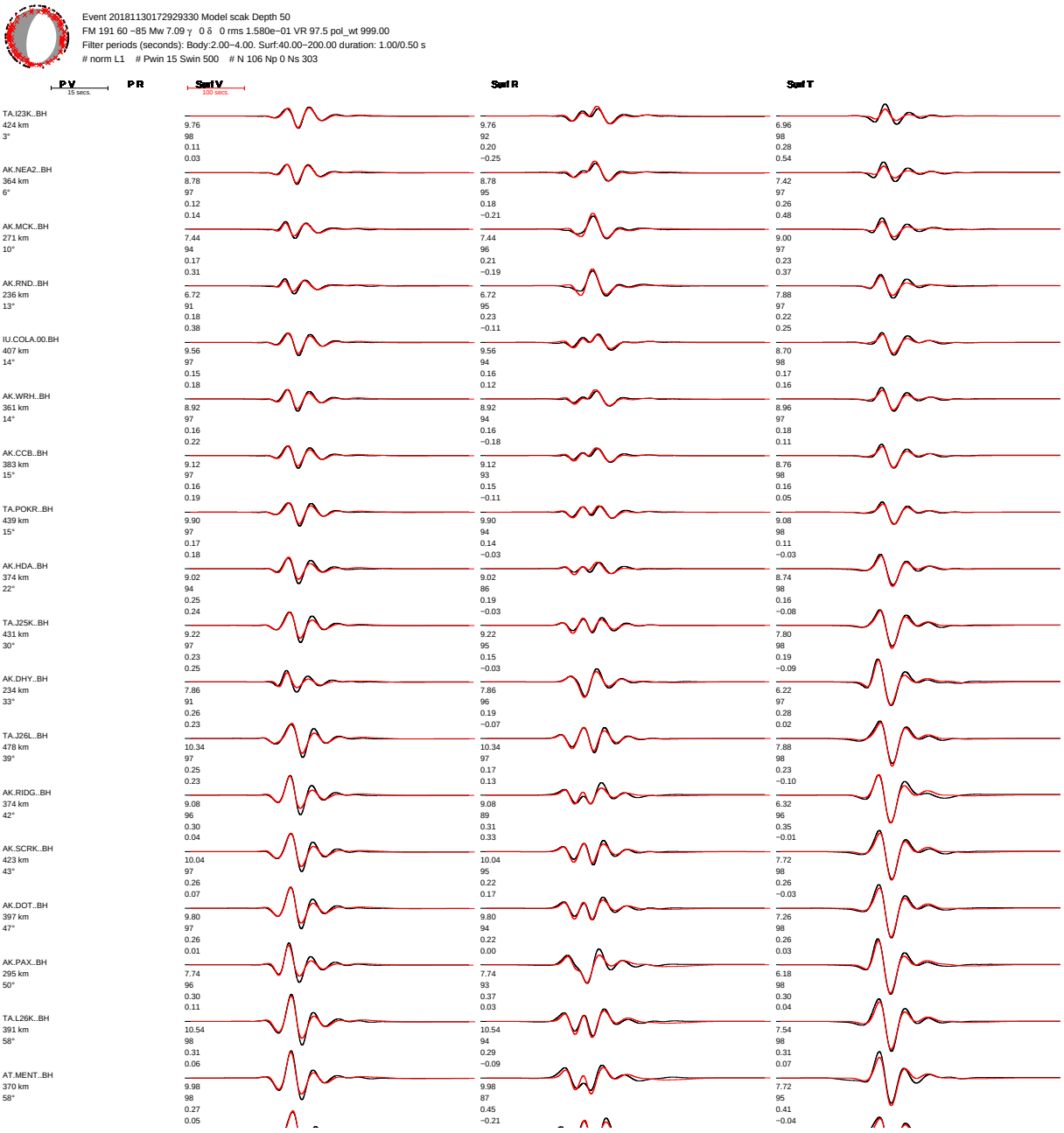

Figure M1: Best-fitting double couple (DC) moment tensor and waveform fits for the 2018-11-30 M_{w} 7.1 Anchorage earthquake. Red = time-shifted synthetics, black = data. For each station, the five time windows are for P wave vertical (PV), P wave radial (PR), Rayleigh waves (Surf V, Surf R), and Love waves (Surf T). Numbers beneath each waveform pair are the time shift, the cross correlation maximum, the percentage of the misfit function, and the log amplitude ratio. Same figure but showing all stations can be found in [`waveform_fits_mshock_DC.pdf`]

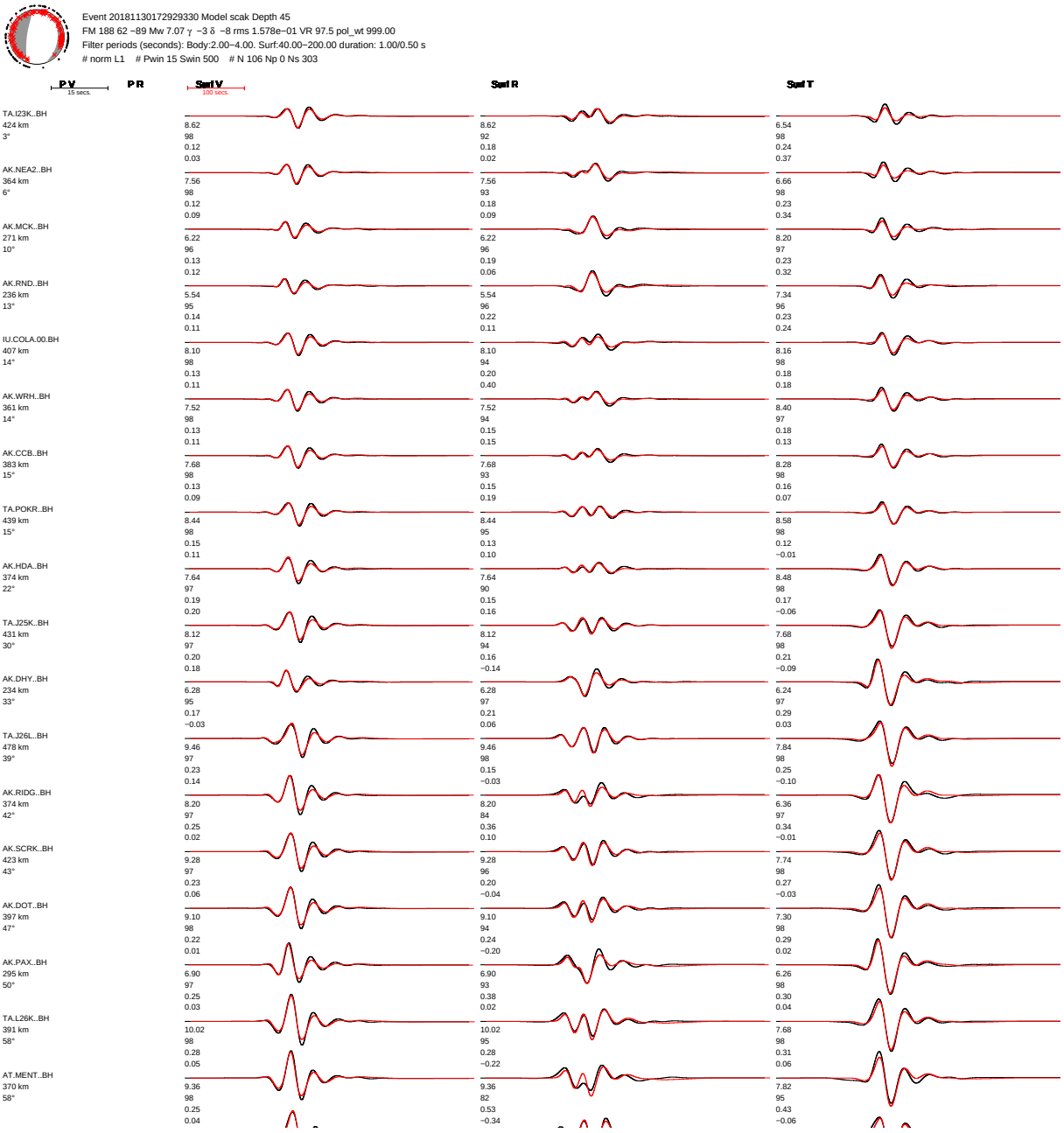

Figure M2: Best-fitting full moment tensor (fmt) and waveform fits for the 2018-11-30 M_{w} 7.1 Anchorage earthquake. Red = time-shifted synthetics, black = data. For each station, the five time windows are for P wave vertical (PV), P wave radial (PR), Rayleigh waves (Surf V, Surf R), and Love waves (Surf T). Numbers beneath each waveform pair are the time shift, the cross correlation maximum, the percentage of the misfit function, and the log amplitude ratio. Same figure but showing all stations can be found in [`waveform_fits_mshock_fmt.pdf`]

(a)

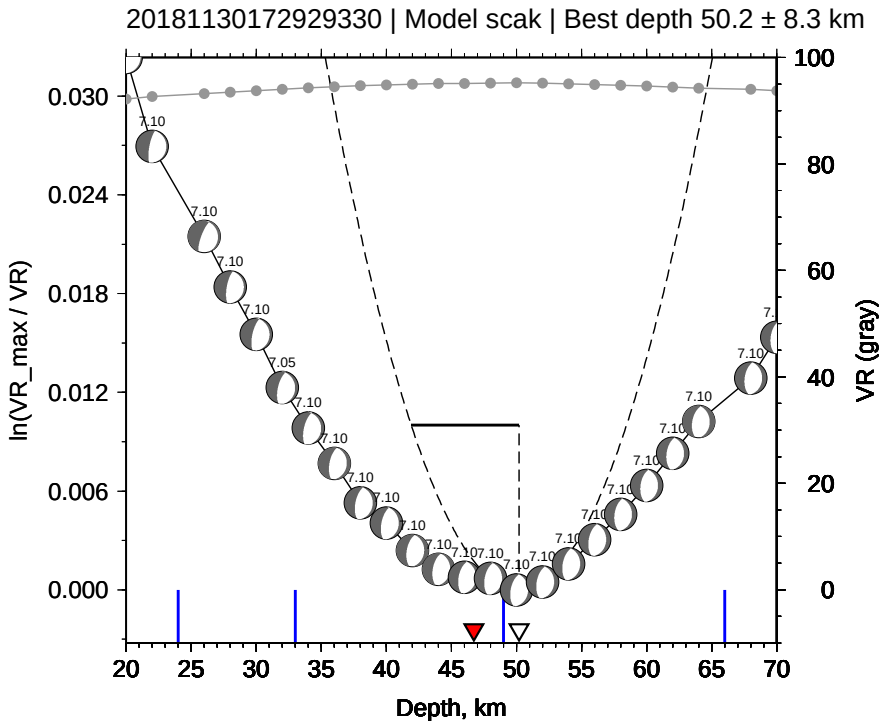

(b)

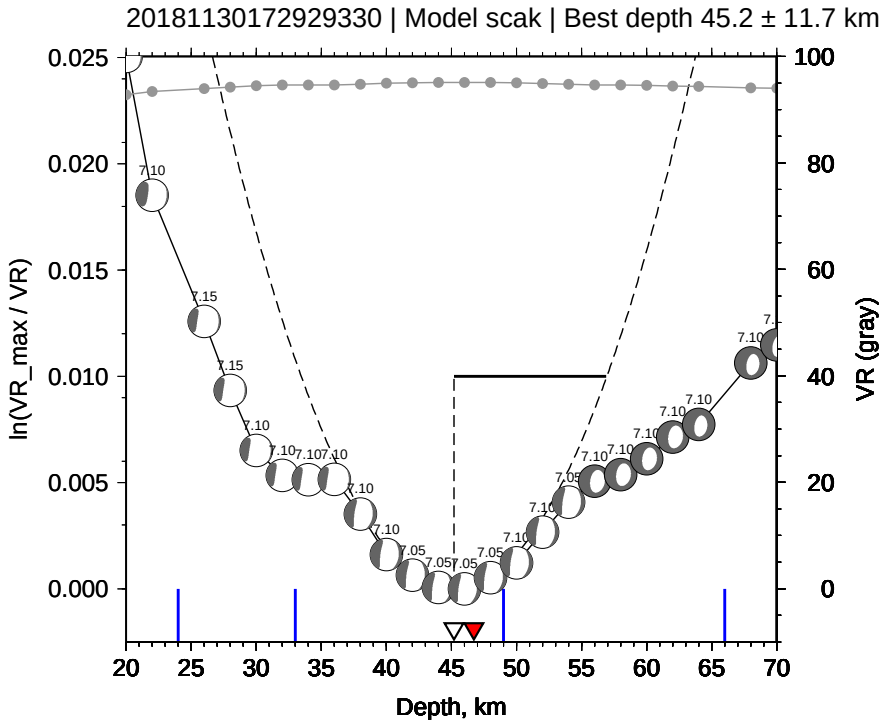

Figure M3: Grid search over depth for moment tensors for the 2018-11-30 M_{w} 7.1 Anchorage earthquake. At each depth, the best-fitting moment tensor (including magnitude) is shown. The magnitude search increment is $\Delta M_{\mathrm{w}} = 0.05$; the depth search increment is 2 km. The red triangle denotes the AEC catalog depth of 46.7 km, which is obtained from P and S arrival times. The blue lines on the x-axis denote the layer boundaries in the 1D velocity model. (a) Double couple constraint. Best-fitting depth is 50.2 ± 8.3 km. (b) Full moment tensor. Best-fitting depth is 45.2 ± 11.7 km. Notice how the source mechanism (and magnitude) changes with depth.

(a)

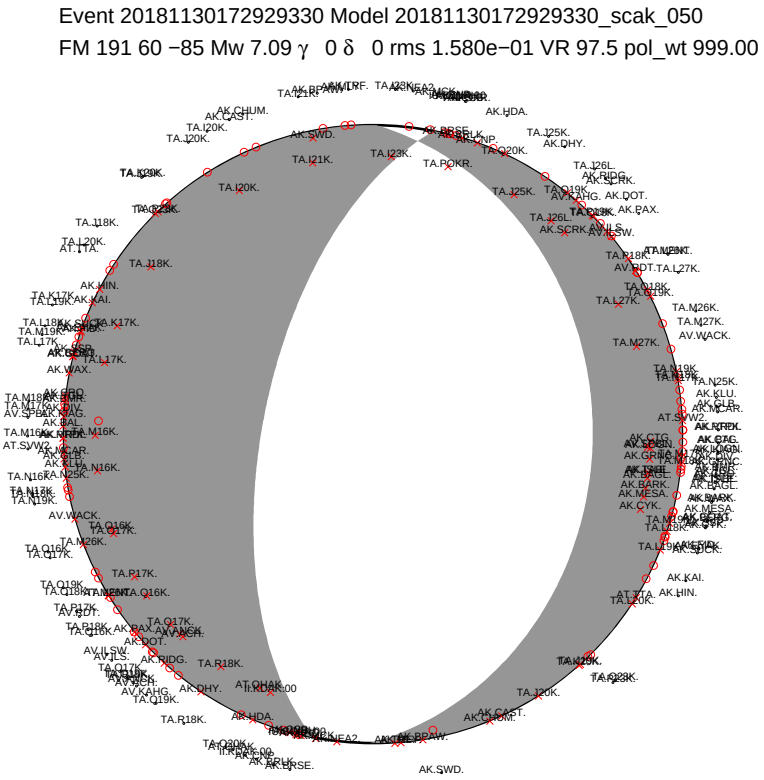

(b)

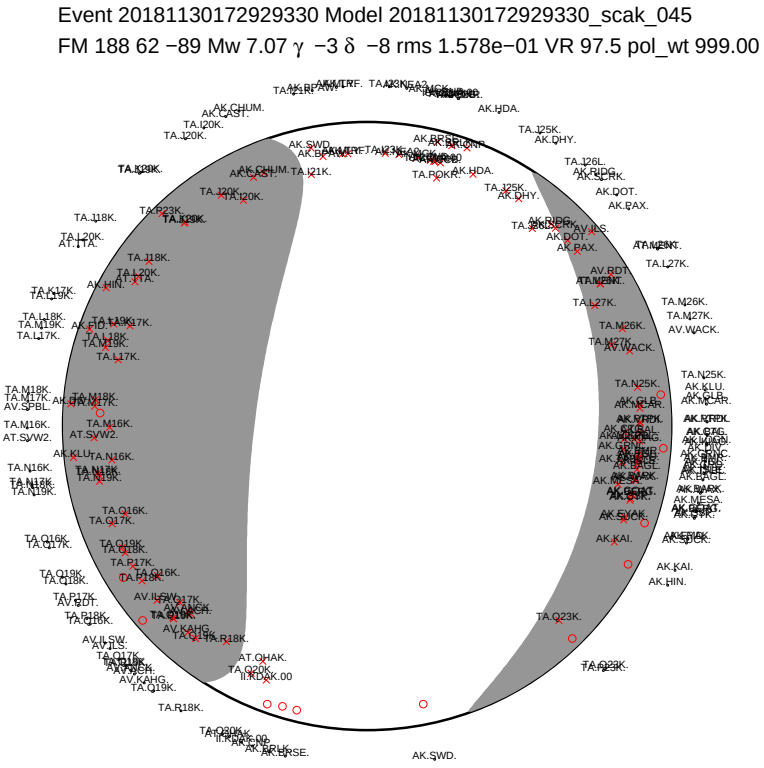

Figure M4: Best-fitting moment tensors for the 2018-11-30 M_{w} 7.1 Anchorage earthquake. The X symbols show the lower-hemisphere piercing points of the ray paths to each station used in the moment tensor search. The text labels on the outside denote the station directions (azimuths) relative to the source. The magnitudes are obtained using an increment of $\Delta M_{\mathrm{w}} = 0.01$, with the depths fixed to the value obtained in Figure M3. (a) Best-fitting double couple moment tensor (M_{w} 7.09, depth 50 km). (b) Best-fitting full moment tensor (M_{w} 7.07, depth 45 km).